

Thermoelectric power of $\text{Ba}(\text{Fe}_{1-x}\text{Ru}_x)_2\text{As}_2$ and $\text{Ba}(\text{Fe}_{1-x}\text{Co}_x)_2\text{As}_2$: Possible changes of Fermi surface with and without changes in electron count

H. Hodovanets, E. D. Mun, A. Thaler, S. L. Bud'ko, and P. C. Canfield

Ames Laboratory, US DOE, and Department of Physics and Astronomy, Iowa State University, Ames, Iowa 50011, USA

(Received 25 October 2010; revised manuscript received 1 December 2010; published 7 March 2011)

Temperature-dependent, in-plane, thermoelectric power (TEP) data are presented for $\text{Ba}(\text{Fe}_{1-x}\text{Ru}_x)_2\text{As}_2$ ($0 \leq x \leq 0.36$) single crystals. The previously outlined x - T phase diagram for this system is confirmed. The analysis of TEP evolution with Ru doping suggests significant changes in the electronic structure, correlations, and/or scattering occurring near $\sim 7\%$, $\sim 30\%$, and possibly $\sim 20\%$ of Ru-doping levels. These results are compared with an extended set of TEP data for the electron-doped $\text{Ba}(\text{Fe}_{1-x}\text{Co}_x)_2\text{As}_2$ series for which initial angle-resolved photoemission spectroscopy and transport studies have identified $x \sim 0.02$ as the concentration at which the Lifshitz transition takes place. In addition to $x \sim 0.02$ the Co levels of $x \approx 0.11$ and 0.22 are identified as concentrations at which similar changes occur.

DOI: [10.1103/PhysRevB.83.094508](https://doi.org/10.1103/PhysRevB.83.094508)

PACS number(s): 74.70.Xa, 72.15.Jf, 71.20.Lp, 74.62.Dh

The recent discovery of families of Fe-As containing materials supporting superconductivity with elevated transition temperatures T_c has attracted the attention of the condensed matter physics community.¹⁻⁴ From the very beginning, details of the electronic structure of these materials were considered to be of importance for magnetism and superconductivity,⁵⁻¹⁷ since in most cases superconductivity was achieved by doping or application of pressure. At least in the particular case of electron doping of the BaFe_2As_2 with a transition metal, it is thought that for superconductivity to appear, the structural/magnetic transition temperature should be suppressed enough *and* the additional electron count caused by doping should be within the certain window.¹⁸⁻²⁰ For the case of the most intensely studied $\text{Ba}(\text{Fe}_{1-x}\text{Co}_x)_2\text{As}_2$ family,²¹⁻²³ the onset of superconductivity was shown^{24,25} to coincide with a Lifshitz transition²⁶ [change of a Fermi surface (FS) topology].

Whereas angle-resolved photoemission spectroscopy (ARPES) or quantum oscillations are extremely important in giving a detailed description of the FS evolution through a Lifshitz transition, in many cases less demanding transport measurements, in particular thermoelectric power, were proven to be very sensitive to the existence of Lifshitz transitions.^{27,28} Indeed, the Hall effect and, more notably, thermoelectric power (TEP) displayed a clear anomaly at the low-doping Lifshitz transition in the $\text{Ba}(\text{Fe}_{1-x}\text{Co}_x)_2\text{As}_2$ and the $\text{Ba}(\text{Fe}_{1-x}\text{Cu}_x)_2\text{As}_2$ series.²⁴ Additionally, in some range of Co concentrations very large, negative (≈ -50 $\mu\text{V}/\text{K}$) TEP values, often associated with a presence of strong electronic correlations, were observed.^{24,29}

In as much as the simple concept of a rigid band appears to give some qualitative understanding of the evolution of physical properties with electron doping, there is less understanding of the salient parameters governing the evolution of the physical properties under pressure or with isoelectronic doping. One of the recent examples of the latter is Ru substitution for Fe in BaFe_2As_2 . Studies by several groups, using single crystals^{30,31} as well as polycrystalline³² samples of $\text{Ba}(\text{Fe}_{1-x}\text{Ru}_x)_2\text{As}_2$, suggest that the structural/magnetic transition is fully suppressed for $x \approx 0.30$, and a superconducting dome with the maximum T_c of ~ 20 K is observed for $0.2 \lesssim x \lesssim 0.4$. An initial band-structural study of Ru

substitution in BaFe_2As_2 ³³ suggested that the qualitative difference between Fermi surfaces of pure BaFe_2As_2 and pure BaRu_2As_2 is the existence of three-dimensional, closed, hole pockets centered near the Z-point in the latter, in contrast to open, corrugated, hole cylinders along Γ -Z in the former. An ARPES study of $\text{Ba}(\text{Fe}_{0.65}\text{Ru}_{0.35})_2\text{As}_2$ resolved several FS pockets but presented no evidence of any topological changes from the parent BaFe_2As_2 compound.³⁴

In this work we present measurements of the in-plane, temperature-dependent TEP on $\text{Ba}(\text{Fe}_{1-x}\text{Ru}_x)_2\text{As}_2$ ($0 \leq x \leq 0.36$) single crystals, with the goals of (i) confirming and refining the x - T phase diagram and (ii) determining the Ru-concentration ranges where significant FS changes may possibly occur. We compare the data for the $\text{Ba}(\text{Fe}_{1-x}\text{Ru}_x)_2\text{As}_2$ series with similar data for the $\text{Ba}(\text{Fe}_{1-x}\text{Co}_x)_2\text{As}_2$ series, here extended to a significantly higher range of Co concentrations. Although ARPES data have confirmed²⁵ the initial identification of a Lifshitz transition from earlier, transport measurements²⁴ on a limited Co range ($x \leq 0.114$), in this study we examine both Ru and Co doping levels up to 0.36 and 0.42 respectively.

Single crystals of $\text{Ba}(\text{Fe}_{1-x}\text{Ru}_x)_2\text{As}_2$ ($0 \leq x \leq 0.36$) and $\text{Ba}(\text{Fe}_{1-x}\text{Co}_x)_2\text{As}_2$ ($0 \leq x \leq 0.42$) were grown out of self-flux using conventional high temperature solution growth techniques, as described in detail in Refs. 22 and 31. Elemental analysis of the single crystals was performed using wavelength dispersive x-ray spectroscopy (WDS) in a JEOL JXA-8200 electron microprobe. Measured (as opposed to nominal) Ru and Co concentrations are used in the text. Physical properties of the majority of the samples in this study were described in detail in previous publications.^{22,31} TEP measurements were carried out by a dc, alternating temperature gradient (two heaters and two thermometers) technique³⁵ over the temperature range between 2 K and 300 K using a Quantum Design PPMS to provide the temperature environment.

Temperature-dependent, in-plane, TEP data for $\text{Ba}(\text{Fe}_{1-x}\text{Ru}_x)_2\text{As}_2$ ($0 \leq x \leq 0.36$) single crystals are shown in Fig. 1. In contrast to $\text{Ba}(\text{Fe}_{1-x}\text{Co}_x)_2\text{As}_2$ (Ref. 24) the absolute values of TEP do not exceed ~ 10 $\mu\text{V}/\text{K}$. For all concentrations measured, a broad minimum is

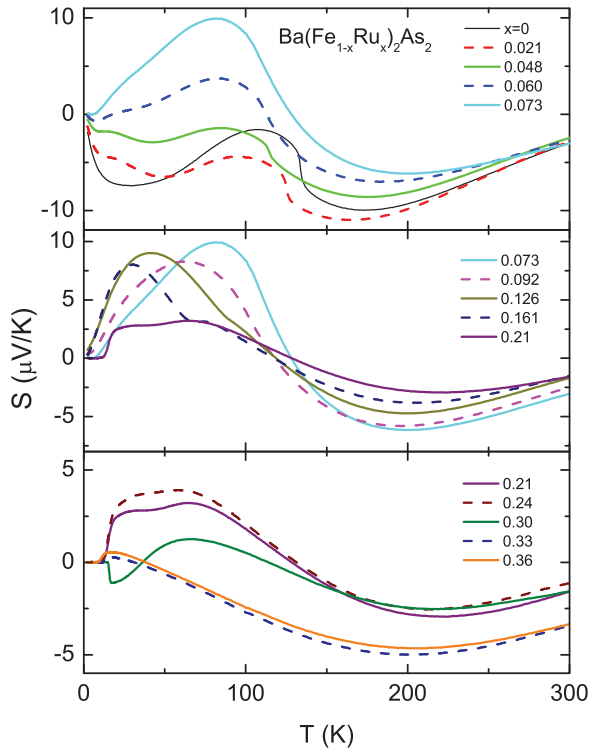


FIG. 1. (Color online) In-plane TEP of the $\text{Ba}(\text{Fe}_{1-x}\text{Ru}_x)_2\text{As}_2$ ($0 \leq x \leq 0.36$) single crystals. The plot is divided into three panels for clarity. The curves for $x = 0.073$ and $x = 0.21$ are each repeated on two panels for continuity.

observed in the 150–200 K temperature range. In addition, multiple, broad, features (the origins of which are unclear at this point) are observed for many Ru concentrations. For $0.21 \leq x \leq 0.36$, zero TEP at low temperatures, corresponding to the superconducting state, is clearly seen in the data. The criteria used for constructing of a x - T phase diagram from the TEP data are shown in Fig. 2. For the structural/magnetic transition an extremum in the derivative dS/dT is used to infer a critical temperature. As already noted from resistance and susceptibility data,³¹ with Ru doping the structural/magnetic transition is suppressed, the characteristic feature broadens, but no signature of split transitions is observed. It is noteworthy that starting from $x = 0.126$, the characteristic feature marking the structural/magnetic transition changes from a local minimum to local maximum [Fig. 2(a)]. For superconducting transitions, an offset criterion [as shown for $x = 0.30$ in Fig. 2(b)] was used to infer T_c . For two concentrations, $x = 0.21$ and 0.24 , $S(T)$ data have a significant shoulder at the superconducting transition. In these two cases two criteria, offset, and $S(T) = 0$ were used [marked by arrows for $x = 0.24$ in Fig. 2(b)]. The phase diagram obtained from the TEP measurements [Fig. 3(a)] is consistent with that reported in Ref. 31: the structural/magnetic transition is suppressed by $x \sim 0.3$ and the superconducting dome exists between approximately $x = 0.2$ and $x = 0.4$.

There are several approaches that allow for the detection of changes in the electronic structure from TEP measurements. TEP at fixed temperature plotted as a function of a control parameter (Ru or Co concentration in our case) is expected to show anomalous behavior at Lifshitz transitions.^{27,28}

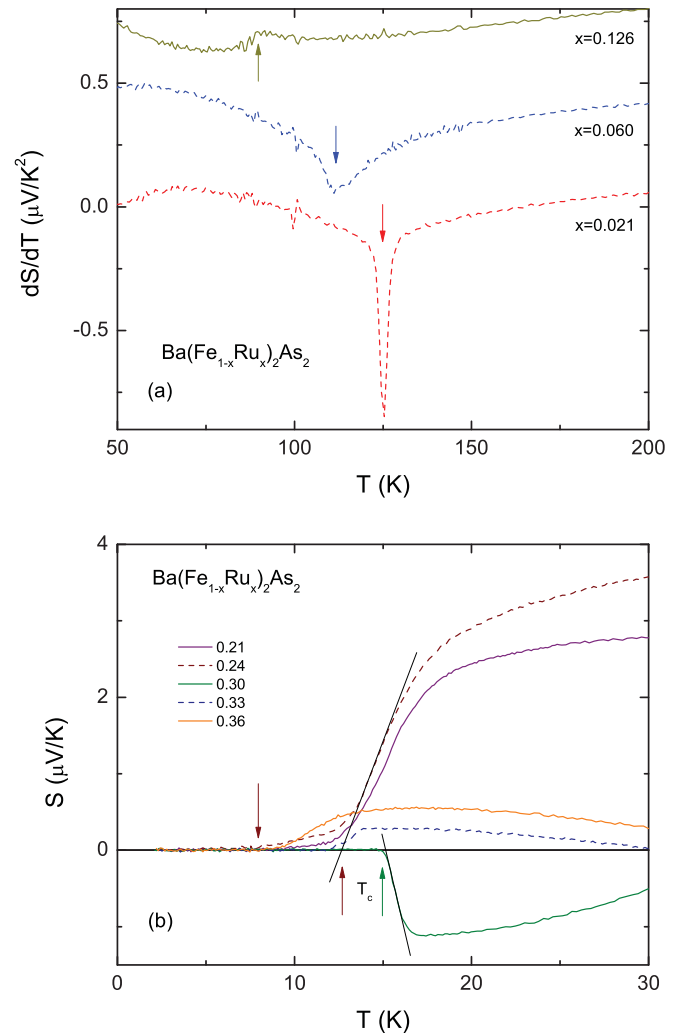


FIG. 2. (Color online) (a) Derivatives dS/dT for representative concentrations, with the structural/magnetic transition temperatures marked with arrows. The data for $x = 0.060$ and $x = 0.126$ are shifted along the y axis by 0.4 and $0.8 \mu\text{V}/\text{K}^2$ for clarity. (b) Low temperature $S(T)$ curves for $0.21 \leq x \leq 0.36$ with the T_c criteria marked with arrows (see text for details).

Figure 3(b) shows the doping dependence of TEP at selected, fixed temperatures. For the three highest Ru concentrations, results from measurements on two samples each are shown. The data for $T = 25$ K and 50 K have a clear feature at $x \sim 0.2$. This feature is weak, but discernible, in the 150 K and 200 K data. It appears to be enhanced in the low temperature $S(x)$ cuts due to crossing of the structural/magnetic transition line [T_s/T_m in Fig. 3(a)]. The data for $T = 150$ K and 200 K correspond to the same, tetragonal structure and absence of the magnetic order. A change in the doping dependence of TEP at selected, fixed temperature, $S(x)|_{T=\text{const}}$, data (for all presented temperatures) is clearly seen at $x \sim 0.07$. Another steplike feature at $x \sim 0.3$ is unambiguous in 150 K and 200 K data and is somewhat obscured, possibly by crossing of the T_s/T_m line, for the low temperature data.

Another approach relies on the analysis of the low temperature, linear in T , coefficient of TEP, S/T (Ref. 36). For a free electron gas, S/T depends on carrier concentration, density

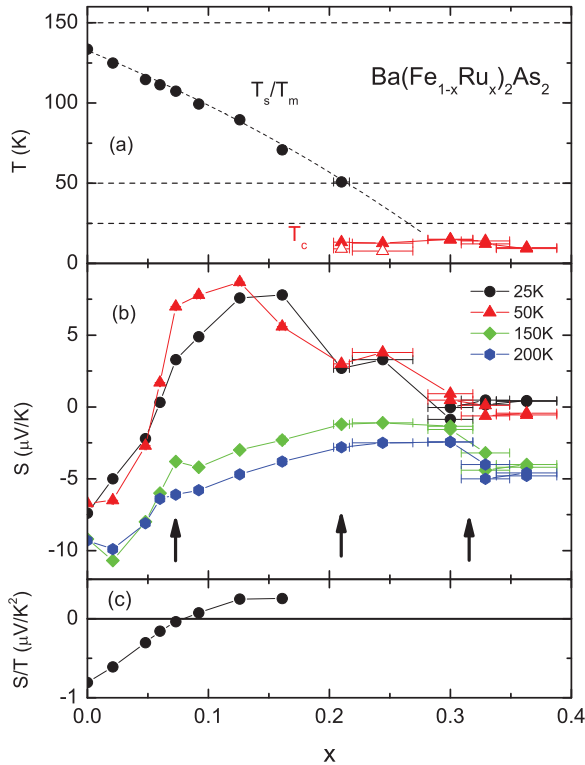


FIG. 3. (Color online) (a) x - T phase diagram for $\text{Ba}(\text{Fe}_{1-x}\text{Ru}_x)_2\text{As}_2$ obtained from the TEP measurements. T_s/T_m denotes the structural/magnetic transition, and T_c , the superconducting transition. The lines through the experimental points are guides for the eye. The criteria used are explained in the text. The open triangles show T_c from $S = 0$ criterion. The horizontal lines correspond to 25, 50, and 150 K. (b) x -dependent TEP of $\text{Ba}(\text{Fe}_{1-x}\text{Ru}_x)_2\text{As}_2$ at fixed, 25, 50, 150, and 200 K temperatures. Arrows mark the regions of anomalous $S(x)|_{T=\text{const}}$ behavior. (c) Low-temperature values of S/T for non-superconducting $\text{Ba}(\text{Fe}_{1-x}\text{Ru}_x)_2\text{As}_2$ samples. Error bars correspond to $\pm\sigma$ (standard deviation) in Ru concentration as determined by WDS. The σ values vary from 0.5×10^{-3} for low Ru dopings to 0.025 at high Ru dopings. See Ref. 31 for details.

of states, and scattering. For real materials the description of TEP becomes very complex. Still, in lieu of comprehensive theory, one can try to look at gross features in S/T as a function of a control parameter. For the non-superconducting $\text{Ba}(\text{Fe}_{1-x}\text{Ru}_x)_2\text{As}_2$ samples the low temperature S/T parameter determined from a linear fit of the $S(T)$ data below ~ 4 K (see Fig. 4) is plotted in Fig. 3(c). The line crosses zero at $x \approx 0.07$, in the same concentration range where an anomaly in $S(x)|_{T=\text{const}}$ is observed.

The results above for the $\text{Ba}(\text{Fe}_{1-x}\text{Ru}_x)_2\text{As}_2$ series can be compared with the TEP data for the well-studied electron-doped $\text{Ba}(\text{Fe}_{1-x}\text{Co}_x)_2\text{As}_2$ series. For such comparison the TEP data for $0 \leq x \leq 0.114$ were taken from the previous publication,²⁴ and new data for $0.13 \leq x \leq 0.42$ (Fig. 5), extending far into the overdoped, non-superconducting range of Co concentrations, were added. It is noteworthy that in this latter, non-superconducting range of Co concentrations the $S(T)$ behavior appears to be qualitatively consistent with that described within a simple two-band 3D model.³⁷ In the overdoped,

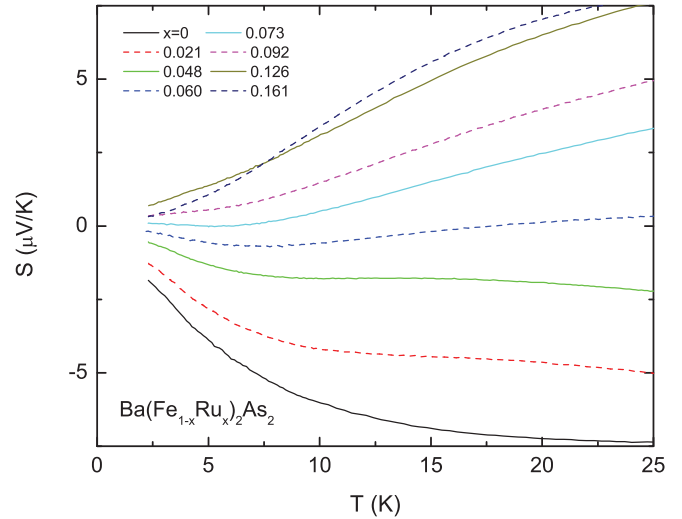


FIG. 4. (Color online) Low temperature part of in-plane TEP of the non-superconducting $\text{Ba}(\text{Fe}_{1-x}\text{Ru}_x)_2\text{As}_2$ ($0 \leq x \leq 0.161$) single crystals.

non-superconducting range of Co concentrations the broad local minimum moves up in temperature, out of the measured temperature range for $x > 0.2$, with no detectable sudden change in the $S(T)$ values. Figure 6 presents a schematic phase diagram for the $\text{Ba}(\text{Fe}_{1-x}\text{Co}_x)_2\text{As}_2$ series, concentration-dependent TEP for 25 K, 50 K, 150 K, and 200 K, and low temperature S/T values for non-superconducting members of the series. The low-concentration Lifshitz transition, discussed at length in previous publications,^{24,25} is clearly seen as an abrupt feature in the $S(x)|_{T=\text{const}}$ data and in an approaching-zero low-temperature S/T value. On further Co doping, two more subtle features are observed in the $S(x)|_{T=\text{const}}$ data, at $x \sim 0.11$ and at $x \sim 0.22$. The possibility of several Lifshitz transitions in Co-doped BaFe_2As_2 was suggested in several experimental and band-structural studies,^{25,38,39,41} broadly speaking, in the $x \sim 0.2$ – 0.3 concentration range. Our TEP data indicate the concentrations ~ 0.1 and ~ 0.2 for further, more careful investigation. Two new lines on the x - T phase diagram of the $\text{Ba}(\text{Fe}_{1-x}\text{Co}_x)_2\text{As}_2$ series

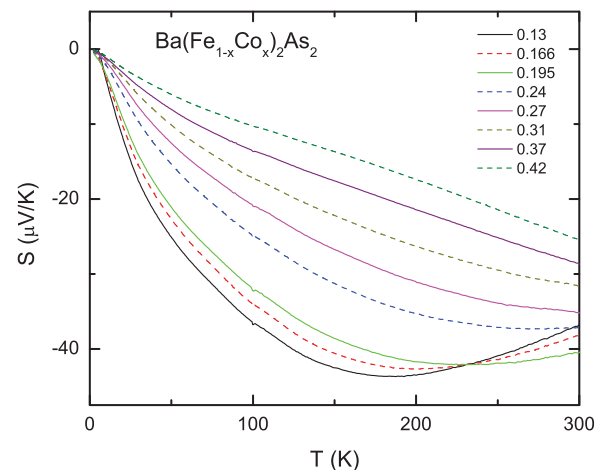


FIG. 5. (Color online) In-plane TEP of the $\text{Ba}(\text{Fe}_{1-x}\text{Co}_x)_2\text{As}_2$ ($0.13 \leq x \leq 0.42$) single crystals.

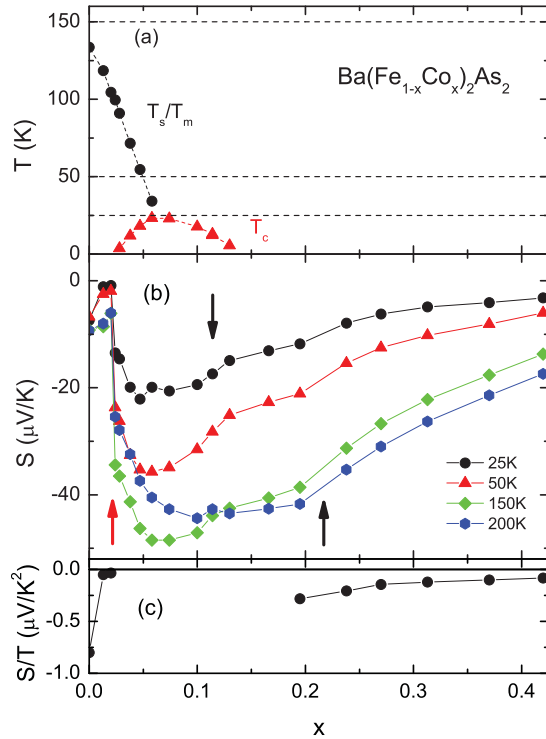


FIG. 6. (Color online) (a) x - T phase diagram for $\text{Ba}(\text{Fe}_{1-x}\text{Co}_x)_2\text{As}_2$ obtained from the TEP measurements. T_s/T_m denotes the structural/magnetic transitions shown here, schematically as a single line; T_c denotes the superconducting transition. Lines through the experimental points are guides for the eye. The criteria used are explained in the text. The horizontal lines correspond to 25, 50, and 150 K. (b) x -dependent TEP of $\text{Ba}(\text{Fe}_{1-x}\text{Co}_x)_2\text{As}_2$ at fixed, 25, 50, 150, and 200 K temperatures. Arrows mark the regions of anomalous $S(x)|_{T=\text{const}}$ behavior. (c) Low-temperature values of S/T for non-superconducting $\text{Ba}(\text{Fe}_{1-x}\text{Co}_x)_2\text{As}_2$ samples.

were suggested based on c -axis resistivity measurements and NMR.⁴⁰ Rather large slopes of these lines are not consistent with observations based on TEP; future $S(T)$ measurements with $\Delta T \parallel c$ may be instrumental for understanding of the origin of these lines.

From this TEP analysis, three ranges of Ru concentrations, $x \sim 0.07$, ~ 0.3 , and possibly ~ 0.2 , are suggested for possible Lifshitz transitions or other drastic changes in electronic structure, correlations, or scattering in $\text{Ba}(\text{Fe}_{1-x}\text{Ru}_x)_2\text{As}_2$. Whereas in $\text{Ba}(\text{Fe}_{1-x}\text{Co}_x)_2\text{As}_2$ the lower concentration Lifshitz transition coincides with the onset of superconductivity, in the case of Ru doping there is no obvious feature in the x - T phase diagram at $x \approx 0.07$. Similarly, Hall and TEP anomalies²⁴ in $\text{Ba}(\text{Fe}_{1-x}\text{Cu}_x)_2\text{As}_2$, which occur at the same

extra electron (e) value as the lower concentration Lifshitz transition in $\text{Ba}(\text{Fe}_{1-x}\text{Co}_x)_2\text{As}_2$, do not signal the occurrence of superconductivity. A change in the Fermi surface topology might be necessary but is not sufficient for superconductivity to occur in BaFe_2As_2 with doping.²⁰ The second anomaly in the TEP of $\text{Ba}(\text{Fe}_{1-x}\text{Ru}_x)_2\text{As}_2$ occurs at the concentration corresponding to complete suppression of the structural/magnetic transition, the maximum of the superconducting dome and linear behavior of the normal state resistivity. Even though the physical picture behind the remarkably similar, anomalous behavior of a number of properties of Fe-As based materials driven to such region of the phase diagram either by different dopings or by pressure is not understood, it is clear that TEP is able to delineate this region as well. For the $\text{Ba}(\text{Fe}_{1-x}\text{Co}_x)_2\text{As}_2$ series, two new anomalies were observed, one in the overdoped half of the superconducting dome on the overdoped side, and another in the non-superconducting, overdoped part of the phase diagram, beyond the dome.

To summarize, the temperature-dependent in-plane TEP in $\text{Ba}(\text{Fe}_{1-x}\text{Ru}_x)_2\text{As}_2$ ($0 \leq x \leq 0.36$) single crystals shows rather complex behavior. The values are notably smaller than those observed in $\text{Ba}(\text{Fe}_{1-x}\text{Co}_x)_2\text{As}_2$ and are more consistent with those expected in normal, weakly correlated metals. The x - T phase diagram obtained from TEP measurements is similar to the one previously outlined.³¹ TEP analysis suggests three concentration ranges, $x \sim 0.07$, $x \sim 0.3$, and possibly $x \sim 0.2$, where Lifshitz transitions or other significant changes of the electronic structure or correlations might occur. Similar analysis of extended TEP data for $\text{Ba}(\text{Fe}_{1-x}\text{Co}_x)_2\text{As}_2$ suggests, in addition to the known Lifshitz transition at $0.020 < x < 0.024$, two other concentration ranges, $x \sim 0.11$ and $x \sim 0.22$, where significant changes of the electronic structure or correlations possibly occur. Detailed experimental (including ARPES and c -axis TEP) and theoretical studies in the vicinity of these critical concentrations are required to shed light on evolution of physical properties of BaFe_2As_2 with isoelectronic doping in comparison to the electron doping. These studies might be relevant for understanding the results obtained under pressure as well.

Ames Laboratory is operated for the US Department of Energy by Iowa State University under Contract No. DE-AC02-07CH11358. This work was supported by the US Department of Energy, Office of Basic Energy Science, Division of Materials Sciences and Engineering. S.L.B. and P.C.C. were supported in part by the State of Iowa through the Iowa State University. Discussions (P.C.C., S.L.B.) about “TEP as a wonder measurement” with Bryan Coles are fondly remembered. The help of A. Kracher and W. E. Straszheim in the elemental analysis of the crystals and of J. Q. Yan, N. Ni, and S. Ran in synthesis is greatly appreciated.

¹J. Phys. Soc. Jpn., *Iron-Pnictide and Related Superconductors Collection*, [http://www.ipap.jp/articles/showArticle.cgi?sec=Fe].

²New J. Phys., *Focus on Iron-Based Superconductors*, edited by Hideo Hosono and Zhi-An Ren, **11**, Issue 2 (2009).

³Physica C, *Superconductivity in Iron-Pnictides*, edited by Paul C. W. Chu, Alexei Koshelev, Wai Kwok, Igor Mazin, Ulrich Welp, and Hai-Hu Wen, **469**, Issues 9-12 (2009).

⁴Supercond. Sci. Technol., *Focus on the Electromagnetic Properties of Iron-based Superconductors*, edited by Ruslan Prozorov, Alex Gurevich, and Graeme Luke, **23**, Number 5 (2010).

⁵M. V. Sadovskii, *Usp. Fiz. Nauk* **178**, 1243 (2008) [*Phys. Usp.* **51**, 1201 (2008)].

⁶A. L. Ivanovskii, *Usp. Fiz. Nauk* **178**, 1273 (2008) [*Phys. Usp.* **51**, 1229 (2008)].

- ⁷Yu. A. Izyumov and E. Z. Kurmaev, *Usp. Fiz. Nauk* **178**, 1307 (2008) [*Phys. Usp.* **51**, 1261 (2008)].
- ⁸Chang Liu *et al.*, *Physica C* **469**, 491 (2009).
- ⁹I. I. Mazin and J. Schmalian, *Physica C* **469**, 614 (2009).
- ¹⁰Amalia I. Coldea, *Philos. Trans. R. Soc. A* **368**, 3503 (2010).
- ¹¹N. Ni, S. Nandi, A. Kreyssig, A. I. Goldman, E. D. Mun, S. L. Bud'ko, and P. C. Canfield, *Phys. Rev. B* **78**, 014523 (2008).
- ¹²Milton S. Torikachvili, Sergey L. Bud'ko, Ni Ni, and Paul C. Canfield, *Phys. Rev. Lett.* **101**, 057006 (2008).
- ¹³A. I. Goldman, D. N. Argyriou, B. Ouladdiaf, T. Chatterji, A. Kreyssig, S. Nandi, N. Ni, S. L. Bud'ko, P. C. Canfield, and R. J. McQueeney, *Phys. Rev. B* **78**, 100506 (2008).
- ¹⁴A. Kreyssig *et al.*, *Phys. Rev. B* **78**, 184517 (2008).
- ¹⁵A. I. Goldman *et al.*, *Phys. Rev. B* **79**, 024513 (2009).
- ¹⁶Chang Liu *et al.*, *Phys. Rev. Lett.* **102**, 167004 (2009).
- ¹⁷P. C. Canfield, S. L. Bud'ko, N. Ni, A. Kreyssig, A. I. Goldman, R. J. McQueeney, M. S. Torikachvili, D. N. Argyriou, G. Luke, and W. Yu, *Physica C* **469**, 404 (2009).
- ¹⁸N. Ni, A. Thaler, A. Kracher, J. Q. Yan, S. L. Budko, and P. C. Canfield, *Phys. Rev. B* **80**, 024511 (2009).
- ¹⁹P. C. Canfield, S. L. Bud'ko, Ni Ni, J. Q. Yan, and A. Kracher, *Phys. Rev. B* **80**, 060501(R) (2009).
- ²⁰Paul C. Canfield and Sergey L. Bud'ko, *Annu. Rev. Condens. Matter Phys.* **1**, 27 (2010).
- ²¹Athena S. Sefat, Rongying Jin, Michael A. McGuire, Brian C. Sales, David J. Singh, and David Mandrus, *Phys. Rev. Lett.* **101**, 117004 (2008).
- ²²N. Ni, M. E. Tillman, J.-Q. Yan, A. Kracher, S. T. Hannahs, S. L. Bud'ko, and P. C. Canfield, *Phys. Rev. B* **78**, 214515 (2008).
- ²³Jiun-Haw Chu, James G. Analytis, Chris Kucharczyk, and Ian R. Fisher, *Phys. Rev. B* **79**, 014506 (2009).
- ²⁴Eun Deok Mun, Sergey L. Bud'ko, Ni Ni, Alex N. Thaler, and Paul C. Canfield, *Phys. Rev. B* **80**, 054517 (2009).
- ²⁵Chang Liu *et al.*, *Nature Phys.* **6**, 419 (2010).
- ²⁶I. M. Lifshitz, *Zh. Eksp. Teor. Fiz.* **30**, 1569 (1960) [*Sov. Phys. JETP* **11**, 1130 (1960)].
- ²⁷A. A. Varlamov, V. S. Egorov, and A. V. Pantsulaya, *Adv. Phys.* **38**, 469 (1989).
- ²⁸Ya. M. Blanter, M. I. Kaganov, A. V. Pantsulaya, and A. A. Varlamov, *Phys. Rep.* **245**, 159 (1994).
- ²⁹Y. J. Yan, X. F. Wang, R. H. Liu, H. Chen, Y. L. Xie, J. J. Ying, and X. H. Chen, *Phys. Rev. B* **81**, 235107 (2010).
- ³⁰F. Rullier-Albenque, D. Colson, A. Forget, P. Thuéry, and S. Poissonnet, *Phys. Rev. B* **81**, 224503 (2010).
- ³¹A. Thaler, N. Ni, A. Kracher, J. Q. Yan, S. L. Bud'ko, and P. C. Canfield, *Phys. Rev. B* **82**, 014534 (2010).
- ³²Shilpam Sharma, A. Bharathi, Sharat Chandra, V. Raghavendra Reddy, S. Paulraj, A. T. Satya, V. S. Sastry, Ajay Gupta, and C. S. Sundar, *Phys. Rev. B* **81**, 174512 (2010).
- ³³Lijun Zhang and D. J. Singh, *Phys. Rev. B* **79**, 174530 (2009).
- ³⁴V. Brouet *et al.*, *Phys. Rev. Lett.* **105**, 087001 (2010).
- ³⁵Eundeok Mun, Sergey L. Bud'ko, Milton S. Torikachvili, and Paul C. Canfield, *Meas. Sci. Technol.* **21**, 055104 (2010).
- ³⁶Kamran Behnia, Didier Jaccard, and Jacques Flouquet, *J. Phys. Condens. Matter* **16**, 5187 (2004).
- ³⁷B. C. Sales, M. A. McGuire, A. S. Sefat, and D. Mandrus, *Physica C* **470**, 304 (2010).
- ³⁸Lei Fang, Huiqian Luo, Peng Cheng, Zhaosheng Wang, Ying Jia, Gang Mu, Bing Shen, I. I. Mazin, Lei Shan, Cong Ren, and Hai-Hu Wen, *Phys. Rev. B* **80**, 140508 (2009).
- ³⁹V. Brouet, M. Marsi, B. Mansart, A. Nicolaou, A. Taleb-Ibrahimi, P. Le Fèvre, F. Bertran, F. Rullier-Albenque, A. Forget, and D. Colson, *Phys. Rev. B* **80**, 165115 (2009).
- ⁴⁰M. A. Tanatar, N. Ni, A. Thaler, S. L. Bud'ko, P. C. Canfield, and R. Prozorov, *Phys. Rev. B* **82**, 134528 (2010).
- ⁴¹Chang Liu *et al.* (unpublished).